DE GRUYTER Nanophotonics 2020; ■■■(■■■): 20200374

Research article

Aditya Tripathi, Sergey Kruk*, Yunfei Shang, Jiajia Zhou, Ivan Kravchenko, Dayong Jin and Yuri Kivshar

Topological nanophotonics for photoluminescence control

https://doi.org/10.1515/nanoph-2020-0374
Received July 4, 2020; accepted August 26, 2020; published online September 15, 2020

Abstract

Objectives: Rare-earth-doped nanocrystals are emerging light sources that can produce tunable emissions in colours and lifetimes, which has been typically achieved in chemistry and material science. However, one important optical challenge – polarization of photoluminescence – remains largely out of control by chemistry methods. Control over photoluminescence polarization can be gained via coupling of emitters to resonant nanostructures such as optical antennas and metasurfaces. However, the resulting polarization is typically sensitive to position disorder of emitters, which is difficult to mitigate.
Methods: Recently, new classes of disorder-immune optical systems have been explored within the framework of topological photonics. Here we explore disorder-robust topological arrays of Mie-resonant nanoparticles for polarization control of photoluminescence of nanocrystals.
Results: We demonstrate polarized emission from rare-earth-doped nanocrystals governed by photonic topological edge states supported by zigzag arrays of dielectric resonators. We verify the topological origin of polarized photoluminescence by comparing emission from nanoparticles coupled to topologically trivial and nontrivial arrays of nanoresonators.
Conclusions: We expect that our results may open a new direction in the study of topology-enable emission properties of topological edge states in many photonic systems.

Keywords: edge states; nanophotonics; polarization control; rare-earth-doped nanocrystals; topological photonics.

1 Introduction

Topological phases of light provide unique opportunities to create photonic systems immune to scattering losses and disorder [1]. Motivated by on-chip applications, there have been efforts to bring topological photonics to the nanoscale. Nanostructures made of high-index dielectric materials with judiciously designed subwavelength resonant elements supporting both electric and magnetic Mie resonances [2] show a special promise for implementations of the topological order for light.

Topological structures have recently been studied as powerful tools for harnessing light emission in various systems with topological orders including lasers [3, 4], quantum light sources [5], and nonlinear frequency converters [6]. In addition, topological photonics holds promise for the development of novel types of light emitters, as it provides a systematic way to control the number and degree of localization of spectrally isolated topologically robust edge and corner states.

Here we uncover another class of nontrivial effects in harnessing light emission with topology. We use topological properties of nanoscale photonic systems to control polarization of PL of rare-earth-doped nanocrystals.

Rare-earth-doped nanocrystals are emerging light sources used for many applications of nanotechnology such as bioimaging, sensing, therapy, display, data

*Corresponding author: Sergey Kruk, Nonlinear Physics Center, Research School of Physics, Australian National University, Canberra, ACT 2601, Australia; and Department of Physics, University of Paderborn, D-33098 Paderborn, Germany, E-mail: sergey.kruk@anu.edu.au. https://orcid.org/0000-0003-0624-4033
Aditya Tripathi, Nonlinear Physics Center, Research School of Physics, Australian National University, Canberra, ACT 2601, Australia; and Department of Physics, Indian Institute of Technology Delhi, New Delhi 110016, India
Yunfei Shang, Jiajia Zhou and Dayong Jin, Institute for Biomedical Materials and Devices (IBMD), University of Technology Sydney, Sydney, NSW 2007, Australia
Ivan Kravchenko, Center for Nanophase Materials Sciences, Oak Ridge National Laboratory, Oak Ridge, TN 37831, USA
Yuri Kivshar, Nonlinear Physics Center, Research School of Physics, Australian National University, Canberra, ACT 2601, Australia

storage, and photonics devices [7, 8]. The applicability of nanocrystals in the aforementioned aspects is determined by human ability to control their performance in diverse optical dimensions including emission color, spectrum, lifetime, intensity, and polarization.

To date, except for polarization, all other optical parameters of the rare-earth-doped nanocrystals have been extensively engineered by chemistry and material science methods [9–12]. Although polarized emission of rare-earth nanocrystals has been observed [13–16] and demonstrated for flow shear tomography [17], the polarization anisotropy was only detectable through spectroscopic measurements from single or aligned crystals, and most commonly, rod-type nanocrystals. This is because the polarization anisotropy is assigned to each splitting transition of rare-earth ions, and it is determined by the site symmetry in a crystal host. The irregular orientation of the crystalline axis will lead to a neutralization effect. The whole-band-based imaging will also neutralize the polarization information, as narrow peaks from 4f-4f rare-earth transitions may have different dipole orientations. A control of the polarization is even more challenging, as a given nanocrystal always has a fixed crystal phase and site symmetry.

To gain a control over polarization of emission, the emitters can be coupled to resonant nanostructures. Coupling of emitters to individual nanoantennas [18–24] and metasurfaces [25–27] has already been explored for control over the polarization of light [28, 29]. However, the resulting polarization of emission depends typically on the specific positioning of emitters. Precise positioning of emitters on nanostructures is challenging, and typically it requires demanding approaches such as atomic force microscopy [30]. In this regard, polarization control that relies on topologically nontrivial optical modes in nanostructures becomes attractive as topology introduces robustness against disorder in positioning. The topological protection offers to mitigate the dependence of the system on the exact position and orientation of emitters.

In this article, we use topological nanophotonics to control the emission polarization of the rare-earth-doped nanocrystals. Specifically, we use zigzag arrays of dielectric nanoresonators hosting topologically nontrivial optical modes that are robust against perturbations of the system [6]. We couple them with Er^{3+}-doped nanocrystals and observe enhanced polarized PL. We reveal that topological edge states can control polarization of emission in an unusual way. Specifically, in the vicinity of topological edge states, the emission becomes linearly polarized reproducing the polarization of topological edge modes. For the arrays with odd number of nanoresonators, the PL emission from two edges is orthogonally polarized, and for the arrays with even number of nanoresonators, the PL emission becomes copolarized, in accordance with the polarization of the topological states. To test the topological origin of the polarized emission, we study topologically trivial arrays and observe in contrast completely depolarized emission.

2 Results and discussion

We use β-$NaErF_4$@$NaYF_4$ core-shell nanocrystals with average diameter of 25 nm, as shown in the TEM image in Figure 1a and in the schematics in Figure 1b. The nanocrystals are synthesized by using the layer epitaxial growth method [31]. When pumped with 976 nm wavelength laser, the nanocrystals produce PL at around 1532 nm wavelength, which corresponds to the Er^{3+} transition: $^4I_{13/2} \rightarrow {}^4I_{15/2}$, as shown with the relevant energy levels in Figure 1c. The geometry of the zigzag nanostructures is chosen such that the wavelength of the topological edge states matches the wavelength of the nanoparticles' PL. In the topological zigzag array, each disk hosts Mie-resonant

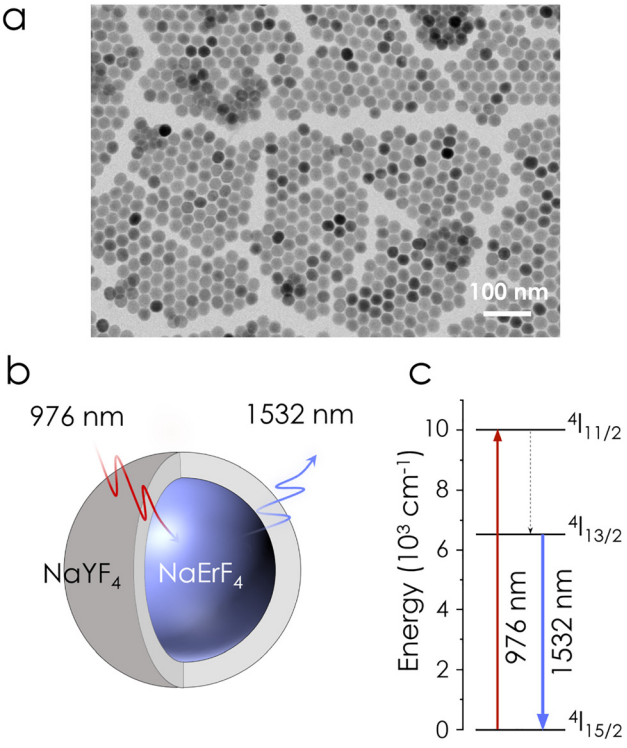

Figure 1: Structure and properties of Er^{3+}-doped core-shell nanoparticles.
(a) Transmission electron microscope image of nanoparticles. (b) Schematic of the core-shell structure of the nanoparticle. (c) Relevant energy levels of Er^{3+}.

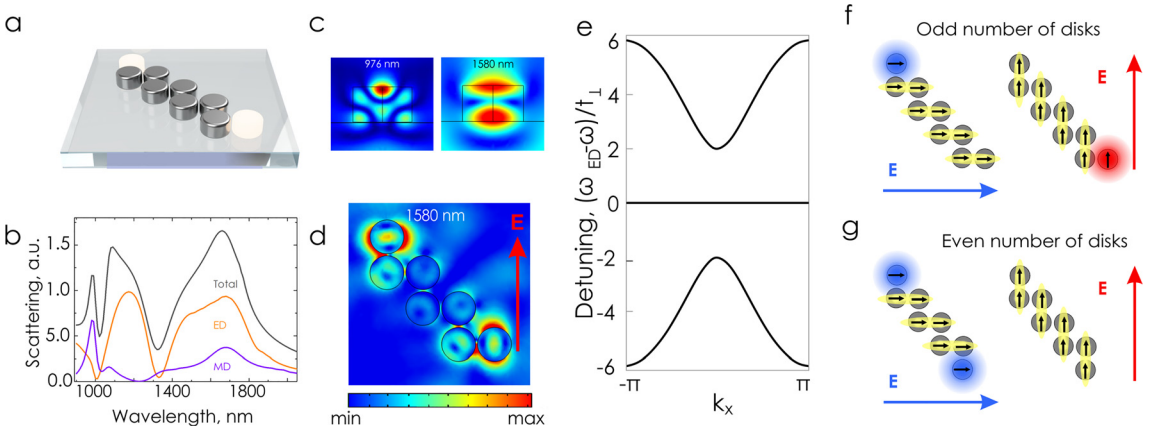

Figure 2: Topological zigzag arrays of dielectric nanoresonators.
(a) Concept image of the zigzag array hosting topological edge states. (b) Multipolar decomposition of a constituent disk nanoresonator. (c) Near-field distributions of a single disk for plane wave excitation at around the pump and the photoluminescence (PL) wavelengths. (d) Full-wave simulation of edge localizations in the zigzag array illuminated with a diagonal polarization. (e) Dispersion curve for Bloch modes in periodic zigzag chain. (f, g) Schematics of the edge states formation in arrays with (f) even and (g) odd number of nanoresonators. The blue and red colors are used to distinguish between two principal polarization of excitation: horizontal and vertical. The yellow joints visualize stronger dipole-dipole coupling between the modes of the near-neighbor disk for the cases of horizontal polarization excitation (left) and vertical polarization excitation (right). Topological states (left side, blue color – horizontally polarized; right side, red color – vertically polarized) form at the edge disks that are weakly coupled to their near-neighbors.

modes [2] (see Figure 2b for details about multipolar expansion and Figure 2c for near-field distributions of the scattered electric field). The electric dipole mode of the disk peaks at around the wavelength of the Er^{3+} electric dipole transition ${}^4I_{13/2} \rightarrow {}^4I_{15/2}$, thus allowing for coupling between the emitter and the nanostructure.

When such nanoresonators are arranged into zigzag arrays, the geometry of the array introduces altered strong and weak near-neighbor coupling which can be described with a polarization-enriched generalized Su-Schrieffer-Heeger–type model [32–34] with a gauge-independent $\mathcal{Z}(2)$ topological invariant. The formation of topologically nontrivial light localization can be described with the analytical coupled dipoles approximation [32]. The Hamiltonian of the system can be written as

$$\mathcal{H} = \sum_{j,v} \hbar\omega_0 a_{jv}^{\dagger} a_{jv} + \sum_{\langle j,j'\rangle,v,v'} a_{jv}^{\dagger} V_{v,v'}^{\langle j,j'\rangle} a_{jv}$$

where ω_0 denotes the resonance frequency, the indices j and j' label the nanoparticles, $\langle j, j'\rangle$ are the first nearest neighbors in the array, and a_{jv} is the annihilation operator for the multipolar eigenmodes with the polarization v at the jth nanoparticle. We consider the electric dipole modes polarized in the plane of the sample (x, y) in either x- or y-directions. The coupling matrices $V^{\langle j,j'\rangle}$ are then written as

$$V^{\langle j,j'\rangle} = t_{\parallel} e_{\parallel}^{\langle j,j'\rangle} \otimes e_{\parallel}^{\langle j,j'\rangle} + t_{\perp} e_{\perp}^{\langle j,j'\rangle} \otimes e_{\perp}^{\langle j,j'\rangle}$$

where $e_{\parallel}^{\langle j,j'\rangle}$ and $e_{\perp}^{\langle j,j'\rangle}$ are the in-plane unit vectors parallel and perpendicular to the vector linking the near-neighbor particles and $t_{\parallel}$ and $t_{\perp}$ are the coupling constants for the modes, copolarized and cross-polarized with respect to the link vector and the $\otimes$ sign stands for the direct product. For short-range dipole-dipole interaction, the ratio of the coupling constants can be estimated as $t_{\parallel}/t_{\perp} = -2$ as shown in the study by Slobozhanyuk et al [32]. Figure 2d shows a full-wave simulation of the edge localizations in the zigzag array.

Figure 2e further visualizes the energy spectrum of the zigzag array of coupled resonators. The spectrum features a band gap with two degenerate edge states associated with the near-field distribution shown in Figure 2d. Nonzero longitudinal components of k-vector were accounted in the coupling constants $t \rightarrow t|2 - e^{ik_x}|$ [6]. The edge-state energy corresponds to the energy of a standalone nanoparticle $\hbar\omega_0$. The resulting topological invariant (winding number) equals 1 within the band gap, which corresponds to the emergence of one polarization-dependent state at every edge [32]. Figure 2f and g visualize resonant coupling of the electric dipole resonant modes of the neighboring nanodisks. Depending on the mutual orientation, the neighboring dipoles couple either strongly (visualized in Figure 2f and g with yellow joints) or weakly. In every case, the weakly coupled edge disk hosts an edge mode.

The resulting edge modes are protected by topology against perturbations of the system such as disorder [6]. The modes are linearly polarized. For arrays with odd number of disks the modes at the opposite ends are

orthogonally polarized (see Figure 2f), and for the even number of disks, the modes are copolarized (see Figure 2g).

We proceed to experiments and fabricate the zigzag arrays of nanoparticles from amorphous silicon on a fused-silica substrate (500 µm thick). First, a 300-nm amorphous silicon layer was deposited onto the substrate by low-pressure chemical vapor deposition. Subsequently, a thin layer of an electron-resist PMMA A4 950 was spin-coated onto the sample, followed by electron beam lithography and development. A thin Cr film was evaporated onto the sample, followed by a lift-of process to generate a hard mask. Reactive-ion etching was used to transfer the Cr mask pattern into the silicon film. The residual Cr mask was removed via wet etching. This resulted in zigzag arrays of disks 510 nm in diameter with 30 nm spacing between the near-neighbors. Finally, Er^{3+}-doped nanocrystals were spin-coated on top of the arrays of dielectric nanoresonators.

In our optical experiments, we pumped the samples with 976 nm CW diode laser. We narrow down the collimated laser output beam with a telescope made of f = 125 mm lens and an objective lens Mitutoyo Plan Apo NIR HR (X100, 0.7NA). We studied spatial distribution of the PL signal in reflection on a camera Xenics Bobcat-320. The resulting measurement is shown in Figure 3a. We next measured PL spectra in reflection with a spectrometer NIR-Quest from Ocean Optics. Figure 3b shows the comparison of a spectrum measured from nanoparticles on a

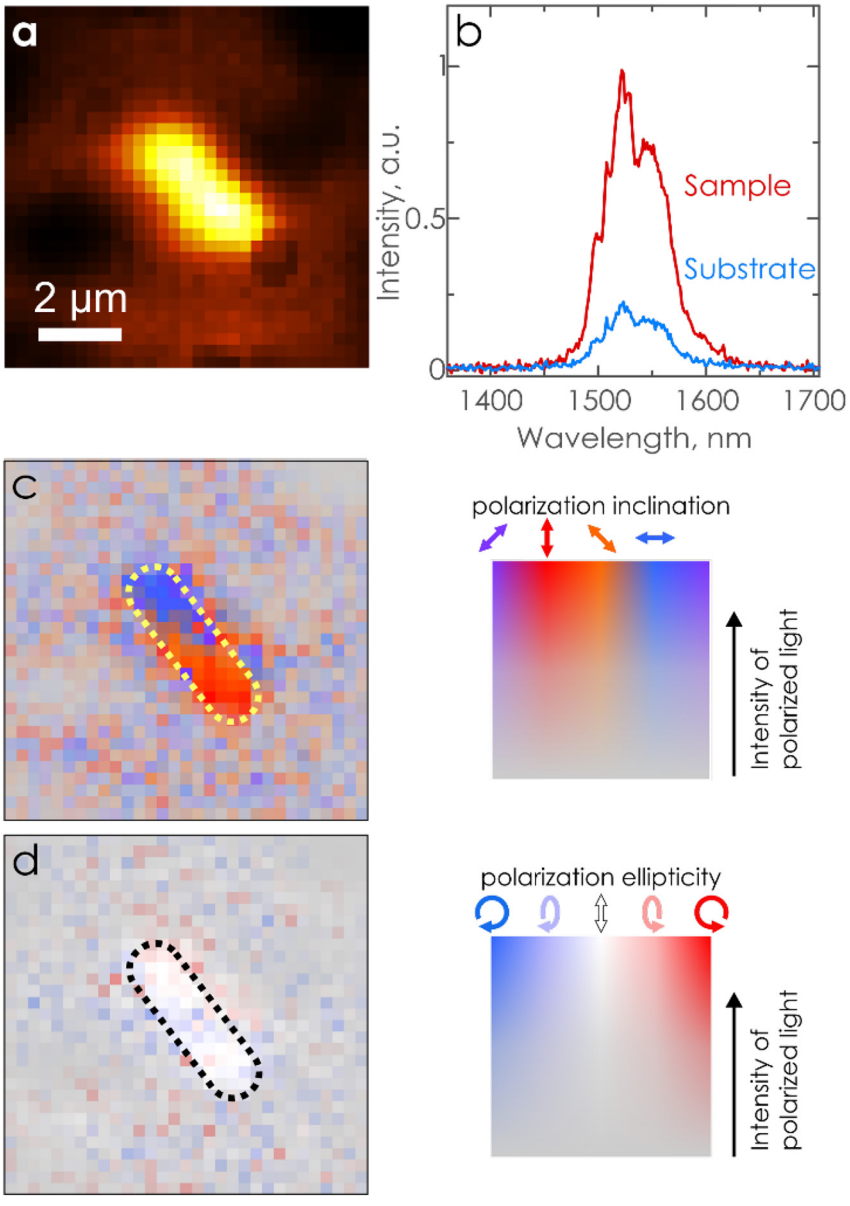

Figure 3: Topology-controlled photoluminescence of Er^{3+} core-shell nanoparticles.
(a) Camera image of the emission enhancement from the Er^{3+} nanoparticles in the vicinity of the zigzag array. (b) Photoluminescence spectra of the Er^{3+} nanoparticles on top of a zigzag array versus on top of a bare substrate. (c, d) Spatially resolved polarization states of photoluminescence showing (c) polarization inclination angles and (d) ellipticity of photoluminescence.

single array with nine nanodisks compared with a spectrum of nanoparticles on a bare glass substrate next to the array. The array provides approximately fivefold enhancement of PL signal.

Next, we experimentally measured spatially resolved polarization states of PL shown in Figure 3c and d. For this, we introduced a quarter-wave plate and a polarizer and performed a Stokes-vector polarimetry. Figure 3c visualizes the polarization inclination angle of PL around the zigzag array. Here, saturation visualizes the intensity of polarized emission (gray – no polarized emission) and the colors visualize the inclination angle of the electric field. Red stands for vertical polarization and blue for horizontal polarization. Figure 3d visualizes ellipticity of emission where similarly saturation reflects the intensity of polarized emission. We notice that ellipticity of polarization is close to zero in all our experiments. We observe that PL from rare-earth-doped nanoparticles becomes polarized in the vicinity of the topological edge states with the polarization state of PL reproducing the polarization of the topological edge mode.

Finally, we compare PL from nanoparticles around the 9-nanodisk zigzag array with 15-nanodisk and 14-nanodisk zigzag arrays as well as with topologically trivial straight array (see Figure 4). The 15-nanodisk zigzag performs qualitatively similar to the 9-nanodisk array as it has same parity of disks (odd). A longer array exhibits sharper localization of the PL as it is expected to provide higher intensity contrast with the bulk [6]. In the 15 disk-long chain PL away from the edge becomes depolarized as the topological modes responsible for polarization control are pinned to the edges. The 14-nanodisk zigzag array in contrast demonstrates copolarized PL in the vicinity of the two edge states in agreement with its parity (even). The bulk of the 15- and 14-nanodisk arrays produces depolarized PL due to lack of polarization sensitivity of zigzag bulk modes. No polarized PL is observed for the topologically trivial array of nanoresonators.

3 Conclusion and outlook

We have studied emission of Er^{3+}-doped nanocrystals deposited on top of topologically nontrivial zigzag arrays of Mie-resonant dielectric nanoparticles. We have observed a novel effect in topological photonics: enhanced and polarized PL emission from the doped nanocrystals located near the topological edge states. We have verified the topological origin of this controlled emission by conducting additional experiments with trivial arrays of the same dielectric nanoresonators, for which we have observed completely depolarized emission.

As the next step in this direction, we expect an efficient control of photon upconversion being crucial for many applications ranging from bioimaging to photovoltaics. By adjusting nanostructure parameters, we expect to achieve a systematical shift of the spectral position of resonances over several hundreds of nanometers, and also observe multifold enhancement of photon upconversion efficiency in nanocrystals which is useful for low-threshold photon upconversion in future solar energy applications.

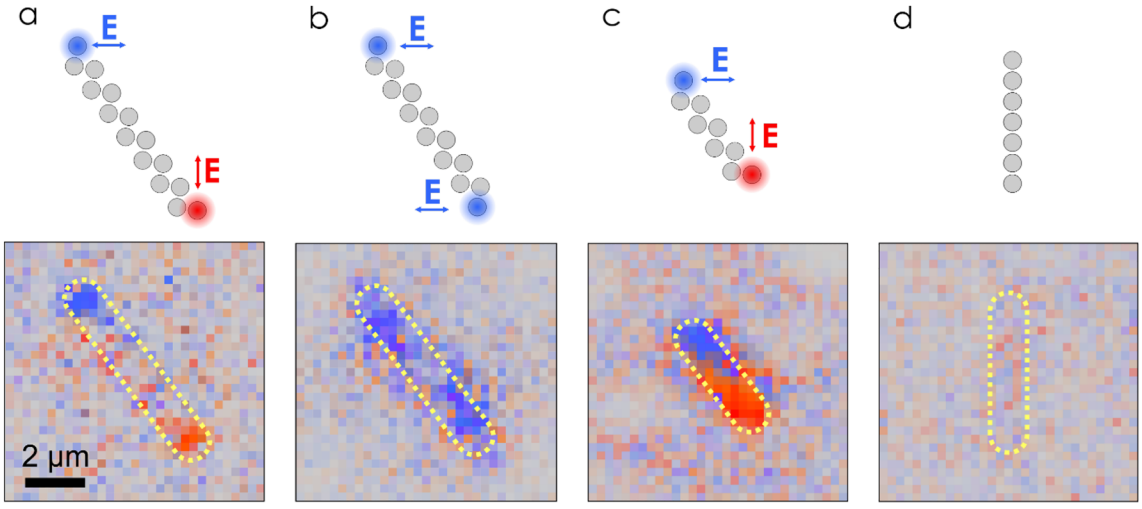

Figure 4: Polarization control of photoluminescence with topological edge states.
Spatially resolved polarization states of photoluminescence for (a) 15-nanodisk zigzag array, (b) 14-nanodisk zigzag array, (c) 9-nanodisk zigzag array, and (d) topologically trivial straight array of resonant nanodisks. The color-map is analogous to that used in Figure 3c.

We expect that our results may open a new direction in the study of topology-enable emission properties of topological edge states in many photonic systems. Indeed, active topological photonics can provide a fertile platform for not only studying interesting fundamental problems involving nontrivial topological phases, but in addition, it may become a route toward the development of novel designs for disorder-immune active photonic device applications, such as robust high-speed routing and switching, nanoscale lasers, and quantum light sources.

Acknowledgments: A part of this research was conducted at the Center for Nanophase Materials Sciences, which is a DOE Office of Science User Facility. A.T. and S.K. thank Barry Luther-Davies for useful discussions and experimental support. S.K. thanks Alexander Poddubny for useful discussions and also acknowledges a financial support from the Alexander von Humboldt Foundation.

Author contribution: All the authors have accepted responsibility for the entire content of this submitted manuscript and approved submission.

Research funding: Australian Research Council (grants DP200101168 and DE180100669), Strategic Fund of the Australian National University, and China Scholarship Council (grant 201706120322).

Conflict of interest statement: The authors declare no conflicts of interest regarding this article.

References

[1] L. Lu, J. D. Joannopoulos, and M. Soljačić, "Topological photonics," *Nat. Photonics*, vol. 8, pp. 821–829, 2014.

[2] Y. Kivshar, "All-dielectric meta-optics and non-linear nanophotonics," *Natl. Sci. Rev.*, vol. 5, pp. 144–158, 2018.

[3] B. Bahari, A. Ndao, F. Vallini, A. El Amili, Y. Fainman, B. Kanté, "Nonreciprocal lasing in topological cavities of arbitrary geometries," *Science*, vol. 358, pp. 636–640, 2017.

[4] M. A. Bandres, S. Wittek, G. Harari, et al., "Topological insulator laser: experiments," *Science*, vol. 359, p. eaar4005, 2018.

[5] S. Barik, A. Karasahin, C. Flower, et al., "A topological quantum optics interface," *Science*, vol. 359, pp. 666–668, 2018.

[6] S. Kruk, A. Poddubny, D. Smirnova, et al., "Nonlinear light generation in topological nanostructures," *Nat. Nanotechnol.*, vol. 14, pp. 126–130, 2019.

[7] B. Zhou, B. Shi, D. Jin, and X. Liu, "Controlling upconversion nanocrystals for emerging applications," *Nat. Nanotechnol.*, vol. 10, pp. 924–936, 2015.

[8] J. Zhou, A. I. Chizhik, S. Chu, and D. Jin, "Single-particle spectroscopy for functional nanomaterials," *Nature*, vol. 579, pp. 41–50, 2020.

[9] F. Wang, R. Deng, J. Wang, et al., "Tuning upconversion through energy migration in core–shell nanoparticles," *Nat. Mater.*, vol. 10, pp. 968–973, 2011.

[10] J. Zhao, D. Jin, E. P. Schartner, et al., "Single-nanocrystal sensitivity achieved by enhanced upconversion luminescence," *Nat. Nanotechnol.*, vol. 8, pp. 729–734, 2013.

[11] Y. Lu, J. Zhao, R. Zhang, et al., "Tunable lifetime multiplexing using luminescent nanocrystals," *Nat. Photonics*, vol. 8, pp. 32–36, 2014.

[12] Y. Fan, P. Wang, Y. Lu, et al., "Lifetime-engineered NIR-II nanoparticles unlock multiplexed in vivo imaging," *Nat. Nanotechnol.*, vol. 13, pp. 941–946, 2018.

[13] J. Zhou, G. Chen, E. Wu, et al., "Ultrasensitive polarized upconversion of Tm^{3+}-Yb^{3+} doped β-$NaYF_4$ single nanorod," *Nano Lett.*, vol. 13, pp. 2241–2246, 2013.

[14] P. Chen, M. Song, E. Wu, et al., "Polarization modulated upconversion luminescence: single particle vs. few-particle aggregates," *Nanoscale*, vol. 7, pp. 6462–6466, 2015.

[15] P. Rodríguez-Sevilla, L. Labrador-Páez, D. Wawrzyńczyk, et al., "Determining the 3D orientation of optically trapped upconverting nanorods by in situ single-particle polarized spectroscopy," *Nanoscale*, vol. 8, pp. 300–308, 2016.

[16] S. Shi, L. D. Sun, Y. X. Xue, et al., "Scalable direct writing of lanthanide-doped $KMnF_3$ perovskite nanowires into aligned arrays with polarized up-conversion emission," *Nano Lett.*, vol. 18, pp. 2964–2969, 2018.

[17] J. Kim, S. Michelin, M. Hilbers, et al., "Monitoring the orientation of rare-earth-doped nanorods for flow shear tomography," *Nat. Nanotechnol.*, vol. 12, pp. 914–919, 2017.

[18] S. Kühn, U. Håkanson, L. Rogobete, and V. Sandoghdar, "Enhancement of single-molecule fluorescence using a gold nanoparticle as an optical nanoantenna," *Phys. Rev. Lett.*, vol. 97, p. 1, 2006.

[19] A. G. Curto, G. Volpe, T. H. Taminiau, et al., "Unidirectional emission of a quantum dot coupled to a nanoantenna," *Science*, vol. 329, pp. 930–933, 2010.

[20] L. Novotny and N. Van Hulst, "Antennas for light," *Nat. Photonics*, vol. 5, pp. 83–90, 2011.

[21] S. S. Kruk, M. Decker, I. Staude, et al., "Spin-polarized photon emission by resonant multipolar nanoantennas," *ACS Photonics*, vol. 1, pp. 1218–1223, 2014.

[22] M. Cotrufo, C. I. Osorio, and A. F. Koenderink, "Spin-dependent emission from arrays of planar chiral nanoantennas due to lattice and localized plasmon resonances," *ACS Nano*, vol. 10, pp. 3389–3397, 2016.

[23] A. Mohtashami, C. I. Osorio, and A. F. Koenderink, "Angle-resolved polarimetry of antenna-mediated fluorescence," *Phys. Rev. Appl.*, vol. 4, p. 23317019, 2015.

[24] C. Yan, X. Wang, T. V. Raziman, and O. J. Martin, "Twisting fluorescence through extrinsic chiral antennas," *Nano Lett.*, vol. 17, pp. 2265–2272, 2017.

[25] S. Luo, Q. Li, Y. Yang, et al., "Controlling fluorescence emission with split-ring-resonator-based plasmonic metasurfaces," *Laser Photonics Rev.*, vol. 11, p. 1770035, 2017.

[26] K. Q. Le, S. Hashiyada, M. Kondo, and H. Okamoto, "Circularly polarized photoluminescence from achiral dye molecules induced by plasmonic two-dimensional chiral nanostructures," *J. Phys. Chem. C*, vol. 122, pp. 24924–24932, 2018.

[27] A. Vaskin, R. Kolkowski, A. F. Koenderink, and I. Staude, "Light-emitting metasurfaces," *Nanophotonics*, vol. 8, pp. 1151–1198, 2019.

[28] K. J. Russell, T. L. Liu, S. Cui, and E. L. Hu, "Large spontaneous emission enhancement in plasmonic nanocavities," *Nat. Photonics*, vol. 6, pp. 459–462, 2012.

[29] K. Y. Bliokh, F. J. Rodríguez-Fortuño, F. Nori, and A. V. Zayats, "Spin-orbit interactions of light," *Nat. Photonics*, vol. 9, pp. 796–808, 2015.
[30] J. V. Chacko, C. Canale, B. Harke, and A. Diaspro, "Sub-diffraction nano manipulation using STED AFM," *PLoS One*, vol. 8, p. 19326203, 2013.
[31] J. Liao, D. Jin, C. Chen, Y. Li, and J. Zhou, "Helix shape power-dependent properties of single upconversion nanoparticles," *J. Phys. Chem. Lett.*, pp. 2883–2890, 2020. https://doi.org/10.1021/acs.jpclett.9b03838.
[32] A. P. Slobozhanyuk, A. N. Poddubny, A. E. Miroshnichenko, P. A. Belov, and Y. S. Kivshar, "Subwavelength topological edge states in optically resonant dielectric structures," *Phys. Rev. Lett.*, vol. 114, p. 123901, 2015.
[33] Y. Hadad, A. B. Khanikaev, and A. Alù, "Self-induced topological transitions and edge states supported by nonlinear staggered potentials," *Phys. Rev. B*, vol. 93, p. 155112, 2016.
[34] S. Kruk, A. Slobozhanyuk, D. Denkova, et al., "Edge states and topological phase transitions in chains of dielectric nanoparticles," *Small*, vol. 13, p. 16136829, 2017.